

## Higher-order elasticity of cubic metals in the embedded-atom method

Somchart Chantasiriwan and Frederick Milstein

*Departments of Materials and Mechanical Engineering, University of California, Santa Barbara, California 93106*

(Received 31 October 1995)

The higher-order elasticity of cubic metals in the framework of the embedded-atom method (EAM) is investigated. Proper groupings of the second- and third-order elastic moduli are shown to yield expressions that depend solely on either the electron density function or the pair potential and which therefore facilitate the construction of EAM models. This formulation also makes evident some important restrictions on the EAM functions and lattice summations. In order for the EAM to model the anharmonic properties accurately, (a) at least the third-nearest-neighbor interactions must be included in the expressions for the cohesive energies of both the body-centered-cubic and face-centered-cubic metals and (b) an electron density function of an inverse power form, as has been employed previously, generally is not valid. Specific EAM models are constructed for a diverse selection of metals (i.e., aluminum, copper, sodium, and molybdenum). These models identically reproduce the respective second- and third-order elastic moduli, as well as the binding energy, atomic volume, unrelaxed vacancy formation energy, and Rose's universal equation of state. They also provide reasonable phonon frequency spectra and structural energy differences

### I. INTRODUCTION

The semiempirical approach to atomistic modeling has been widely used in the study of condensed matter. Most applications involve relatively large, complex, displacements of atoms from their equilibrium positions in the unstressed perfect crystal. Phenomena of interest include the formations and configurations of crystalline defects,<sup>1</sup> lattice deformation and stability at finite strain,<sup>2</sup> and bifurcations and structural transitions of crystals under load.<sup>3</sup> Computational results are likely to be enhanced by use of an atomic model that displays the appropriate harmonic and anharmonic, anisotropic, elastic behavior of the parent crystal, i.e., that accurately reflects both the second- and third-order elastic moduli of the material under consideration.

The present work explores the higher-order elasticity of cubic metals in the framework of a particularly popular semiempirical modeling technique, i.e., the embedded-atom method (EAM). Formulas are given for computing the third-order elastic moduli (TOEM) in general EAM formulations; expressions for the second-order elastic moduli have previously appeared in the literature.<sup>4</sup> The elastic moduli are then grouped in relations that are shown to depend solely on either the electron density function or the pair potential function. These expressions greatly facilitate the construction of any EAM models that incorporate data of the TOEM of cubic crystals. It is further demonstrated that the EAM is capable of exhibiting all of the second- and third-order elastic moduli subject to certain restrictions upon the EAM functions and lattice summations; e.g., (at least) the third-nearest-neighbor interactions must be included in the expression for cohesive energy. As examples of the use of these relations, specific models are constructed for the face-centered-cubic (fcc) metals Al and Cu and the body-centered-cubic (bcc) metals Na and Mo. These metals were selected because each has a characteristically different elastic response to load, and when considered as a group, their responses included those that are typical of cubic metals (this is explained later in Sec.

V). The empirical input data consist of the second-order elastic moduli, third-order elastic moduli, lattice constant at zero pressure, cohesive energy, unrelaxed vacancy formation energy, and Rose's universal equation of state.<sup>5</sup> Finally, these models are shown to give relatively good descriptions of phonon frequency spectra.

Initial attempts to model metals semiempirically made use of pair potentials, which are particularly efficient computationally. While this approach has been found capable of reproducing the salient trends of the linear elastic behavior of crystals (e.g., the algebraic signs of Poisson's ratios and the orderings of the magnitudes of the shear moduli, Young's moduli, and Poisson's ratios associated with major crystallographic symmetries),<sup>6</sup> it is lacking in a strong theoretical justification. In addition, any pair potential model yields certain unphysical conditions (e.g., the Cauchy symmetries among the elastic moduli and an unrelaxed vacancy formation energy that is equal to the cohesive energy).

In recent years, considerable effort has been directed toward the development of atomistic models that retain much of the essential simplicity and mathematical tractability of the pair potentials and also provide a more realistic and accurate description of the relevant energetics. One example, which for simple metals finds justification in pseudopotential theory,<sup>7</sup> is the addition of a purely volume-dependent term to the summation of pairwise potential interactions. While this approach is useful for the study of "bulk properties,"<sup>7,8</sup> and it removes the Cauchy symmetries, the explicit volume dependence entails ambiguities at surfaces or near defects. Furthermore, as noted by Cousins and Martin,<sup>9</sup> an energy expression consisting of only a pair potential and a volume-dependent term still imposes physically unrealistic restrictions upon third-order elastic moduli.

Another computationally efficient approach that is capable of circumventing such limitations is the embedded-atom method. Since its introduction,<sup>10</sup> the EAM has found numerous applications, including phonons, thermodynamic functions, liquid metals, defects, grain boundary structure,

alloys, interdiffusion in alloys, segregation to surfaces and grain boundaries, fracture, and mechanical properties; Ref. 11 contains a comprehensive review. It has been observed that the EAM deals with transition metals with nearly filled or nearly empty  $d$  bands quite well. In addition, a number of EAM models have been proposed for the bcc transition metals<sup>12–15</sup> (although, as is often mentioned, with somewhat less theoretical justification).

The general expression for the configurational cohesive energy per atom,  $E$ , in a homogeneous crystal according to the EAM is

$$E = F(\rho) + \frac{1}{2} \sum_{i \neq j} \phi(r_{ij}), \quad (1a)$$

with

$$\rho = \sum_{i \neq j} f(r_{ij}), \quad (1b)$$

where  $F(\rho)$  is the embedding function,  $\rho$  is the total electron density at the reference atomic site,  $f(r_{ij})$  is the electron density function,  $\phi(r_{ij})$  is the pair potential function, and  $r_{ij}$  is the distance between atoms  $i$  and  $j$ . In principle, EAM functions can be determined from first principles,<sup>16</sup> but in practice, they are invariably determined semiempirically. Thus numerous EAM functions and fitting schemes for incorporating empirical data have appeared in the literature. In this respect, it is important to note that the TOEM render restrictions that are useful in ‘‘narrowing the field.’’

In modeling metals of cubic symmetry, on which this paper is focused, the physical properties to which most EAM functions have been fitted are the lattice constant, the cohesive energy, the unrelaxed vacancy formation energy, and the three second-order elastic moduli. In some cases, the embedding function  $F(\rho)$  is also made to conform to Rose’s universal equation of state<sup>5</sup> to improve the ability of the model to describe the volume-dependent anharmonic properties of the metal (however, this approach does not incorporate empirical anisotropic anharmonic data). Thus, a typical EAM model is fitted to physical properties that depend on up to second derivatives of the configurational energy with respect to *arbitrary*, homogeneous, lattice strains. Such procedures have yielded efficacious EAM models of metals; as mentioned earlier, further enhancement attaches to models that also describe fully the physical properties that depend on the third derivatives of energy with respect to arbitrary homogeneous lattice strains, i.e., the third-order elastic moduli.

The following sections examine the roles of the component parts of the EAM in the description of the TOEM. These sections also comprise a formalism for incorporating the TOEM in the EAM. Section II contains the general formulas for the elastic moduli within the EAM framework. Section III shows how the proper groupings of the elastic moduli can lead to independent determinations of the pair potential  $\phi(r)$  and the electron density function  $f(r)$ . In Sec. IV, we suggest particular model functions  $\phi(r)$  and  $f(r)$ , which have the capability of yielding embedded-atom models with the correct elastic properties; the determination of the remaining EAM function  $F(\rho)$  is also discussed. Sections II–IV constitute a methodology that can be applied to cubic metals in general. Finally, in Sec. V, we apply this

procedure to the construction of specific EAM models for Al, Cu, Na, and Mo, and use these models to calculate phonon frequency spectra and structural energy differences.

## II. THIRD-ORDER ELASTIC MODULI

For a crystal of cubic symmetry, there are six independent TOEM:  $C_{111}$ ,  $C_{112}$ ,  $C_{123}$ ,  $C_{144}$ ,  $C_{166}$ , and  $C_{456}$ . The definition of elastic moduli widely used in the literature was given by Brugger.<sup>17</sup> Within the potential approximation, one considers the elastic free energy per unit mass,  $G(\eta)$ , to depend on only the Lagrangian strain matrix  $\eta_{ij}$ . The Taylor series expansion of  $G(\eta)$  about the unstressed state, which will be referred to below as the reference state, results in

$$\begin{aligned} \rho_0 G(\eta) = & \rho_0 G(0) + \frac{1}{2} c_{ijkl} \eta_{ij} \eta_{kl} \\ & + \frac{1}{6} c_{ijklmn} \eta_{ij} \eta_{kl} \eta_{mn} + \dots, \end{aligned} \quad (2)$$

where  $\rho_0$  is the density at the reference state and the standard summation convention is employed ( $i, j, k, l = 1, 2, 3$ ). If we now use the Voigt notation in replacing  $c_{1122}$  with  $C_{12}$ ,  $c_{112233}$  with  $C_{123}$ ,  $\eta_{11}$  with  $\eta_1$ ;  $2\eta_{23}$  with  $\eta_4$ , etc., then

$$\begin{aligned} \rho_0 G(\eta) = & \rho_0 G(0) + \frac{1}{2} \sum_{I=1}^6 C_{II} \eta_I^2 + \sum_{I < J} C_{IJ} \eta_I \eta_J \\ & + \frac{1}{6} \sum_{I=1}^6 C_{III} \eta_I^3 + \frac{1}{2} \sum_{I \neq J} C_{IJJ} \eta_I \eta_J^2 \\ & + \sum_{I < J < K} C_{IJK} \eta_I \eta_J \eta_K + \dots. \end{aligned} \quad (3)$$

Correspondingly,  $n$ th-order elastic moduli  $C_{IJKL\dots}$  are defined as

$$C_{IJK\dots} = \frac{1}{\Omega_0} \left( \frac{\partial^n G}{\partial \eta_I \partial \eta_J \partial \eta_K \dots} \right), \quad (4)$$

where  $\Omega_0$  is the volume per atom at the reference state. Here the elastic energy  $G$  is simply the configurational energy  $E$  in the EAM format. To evaluate the above derivatives, the  $\partial/\partial \eta_I$  are expressed in terms of  $\partial/\partial r$ , with  $r$  being the distance between lattice points in the crystal. If  $\vec{r} = x_1 \vec{i} + x_2 \vec{j} + x_3 \vec{k}$  and  $\vec{r}_0$  are lattice vectors in the strained and unstrained crystals, respectively, with  $x_i$  representing the Cartesian component of  $\vec{r}$  in the  $i$ th direction, then the difference in their magnitudes is given by

$$r^2 - r_0^2 = 2 \sum_{I=1}^6 X_I \eta_I, \quad (5)$$

where  $X_I = x_i x_j$  and  $I$  is the Voigt contraction of  $ij$ . Second- and third-order elastic moduli within the EAM framework are then written as

$$\Omega_0 C_{IJ} = F'' \left( \sum \frac{X_I f'}{r} \right) \left( \sum \frac{X_J f'}{r} \right) + F' \sum \frac{X_I X_J}{r^2} \left( f'' - \frac{f'}{r} \right) + \frac{1}{2} \sum \frac{X_I X_J}{r^2} \left( \phi'' - \frac{\phi'}{r} \right), \quad (6)$$

$$\begin{aligned} \Omega_0 C_{IJK} = & F''' \left( \sum \frac{X_I f'}{r} \right) \left( \sum \frac{X_J f'}{r} \right) \left( \sum \frac{X_K f'}{r} \right) + F'' \left( \sum \frac{X_I f'}{r} \right) \left[ \sum \frac{X_J X_K}{r^2} \left( f'' - \frac{f'}{r} \right) \right] \\ & + F'' \left( \sum \frac{X_J f'}{r} \right) \left[ \sum \frac{X_I X_K}{r^2} \left( f'' - \frac{f'}{r} \right) \right] + F'' \left( \sum \frac{X_K f'}{r} \right) \left[ \sum \frac{X_I X_J}{r^2} \left( f'' - \frac{f'}{r} \right) \right] \\ & + F' \sum \frac{X_I X_J X_K}{r^3} \left( f''' - 3 \frac{f''}{r} + 3 \frac{f'}{r^2} \right) + \frac{1}{2} \sum \frac{X_I X_J X_K}{r^3} \left( \phi''' - 3 \frac{\phi''}{r} + 3 \frac{\phi'}{r^2} \right), \end{aligned} \quad (7)$$

where the primes on the  $F$  and  $f$  functions represent derivatives with respect to  $\rho$  and  $r$ , respectively. For a crystal of cubic symmetry, the expressions for the three independent second-order elastic moduli are

$$\Omega_0 C_{11} = F'' \left( \sum \frac{x_1^2 f'}{r} \right)^2 + F' \sum \frac{x_1^4}{r^2} \left( f'' - \frac{f'}{r} \right) + \frac{1}{2} \sum \frac{x_1^4}{r^2} \left( \phi'' - \frac{\phi'}{r} \right), \quad (8)$$

$$\Omega_0 C_{12} = F'' \left( \sum \frac{x_1^2 f'}{r} \right)^2 + F' \sum \frac{x_1^2 x_2^2}{r} \left( f'' - \frac{f'}{r} \right) + \frac{1}{2} \sum \frac{x_1^2 x_2^2}{r^2} \left( \phi'' - \frac{\phi'}{r} \right), \quad (9)$$

$$\Omega_0 C_{44} = F' \sum \frac{x_1^2 x_2^2}{r^2} \left( f'' - \frac{f'}{r} \right) + \frac{1}{2} \sum \frac{x_1^2 x_2^2}{r^2} \left( \phi'' - \frac{\phi'}{r} \right), \quad (10)$$

and, for the six independent third-order elastic moduli,

$$\Omega_0 C_{111} = F''' \left( \sum \frac{x_1^2 f'}{r} \right)^3 + 3F'' \left( \sum \frac{x_1^2 f'}{r} \right) \left[ \sum \frac{x_1^4}{r^2} \left( f'' - \frac{f'}{r} \right) \right] + F' \sum \frac{x_1^6}{r^3} \left( f''' - 3 \frac{f''}{r} + 3 \frac{f'}{r^2} \right) + \frac{1}{2} \sum \frac{x_1^6}{r^3} \left( \phi''' - 3 \frac{\phi''}{r} + 3 \frac{\phi'}{r^2} \right), \quad (11)$$

$$\begin{aligned} \Omega_0 C_{112} = & F''' \left( \sum \frac{x_1^2 f'}{r} \right)^3 + F'' \left( \sum \frac{x_1^2 f'}{r} \right) \left[ \sum \frac{x_1^4}{r^2} \left( f'' - \frac{f'}{r} \right) \right] + 2F'' \left( \sum \frac{x_1^2 f'}{r} \right) \left[ \sum \frac{x_1^2 x_2^2}{r^2} \left( f'' - \frac{f'}{r} \right) \right] \\ & + F' \sum \frac{x_1^4 x_2^2}{r^3} \left( f''' - 3 \frac{f''}{r} + 3 \frac{f'}{r^2} \right) + \frac{1}{2} \sum \frac{x_1^4 x_2^2}{r^3} \left( \phi''' - 3 \frac{\phi''}{r} + 3 \frac{\phi'}{r^2} \right), \end{aligned} \quad (12)$$

$$\begin{aligned} \Omega_0 C_{123} = & F''' \left( \sum \frac{x_1^2 f'}{r} \right)^3 + 3F'' \left( \sum \frac{x_1^2 f'}{r} \right) \left[ \sum \frac{x_1^2 x_2^2}{r^2} \left( f'' - \frac{f'}{r} \right) \right] + F' \sum \frac{x_1^2 x_2^2 x_3^2}{r^3} \left( f''' - 3 \frac{f''}{r} + 3 \frac{f'}{r^2} \right) \\ & + \frac{1}{2} \sum \frac{x_1^2 x_2^2 x_3^2}{r^3} \left( \phi''' - 3 \frac{\phi''}{r} + 3 \frac{\phi'}{r^2} \right), \end{aligned} \quad (13)$$

$$\Omega_0 C_{144} = F'' \left( \sum \frac{x_1^2 f'}{r} \right) \left[ \sum \frac{x_1^2 x_2^2}{r^2} \left( f'' - \frac{f'}{r} \right) \right] + F' \sum \frac{x_1^2 x_2^2 x_3^2}{r^3} \left( f''' - 3 \frac{f''}{r} + 3 \frac{f'}{r^2} \right) + \frac{1}{2} \sum \frac{x_1^2 x_2^2 x_3^2}{r^3} \left( \phi''' - 3 \frac{\phi''}{r} + 3 \frac{\phi'}{r^2} \right), \quad (14)$$

$$\Omega_0 C_{166} = F'' \left( \sum \frac{x_1^2 f'}{r} \right) \left[ \sum \frac{x_1^2 x_2^2}{r^2} \left( f'' - \frac{f'}{r} \right) \right] + F' \sum \frac{x_1^4 x_2^2}{r^3} \left( f''' - 3 \frac{f''}{r} + 3 \frac{f'}{r^2} \right) + \frac{1}{2} \sum \frac{x_1^4 x_2^2}{r^3} \left( \phi''' - 3 \frac{\phi''}{r} + 3 \frac{\phi'}{r^2} \right), \quad (15)$$

$$\Omega_0 C_{456} = F' \sum \frac{x_1^2 x_2^2 x_3^2}{r^3} \left( f''' - 3 \frac{f''}{r} + 3 \frac{f'}{r^2} \right) + \frac{1}{2} \sum \frac{x_1^2 x_2^2 x_3^2}{r^3} \left( \phi''' - 3 \frac{\phi''}{r} + 3 \frac{\phi'}{r^2} \right). \quad (16)$$

The summations in Eqs. (6)–(16) are understood to be taken over atoms  $j$  around the reference atom  $i$  ( $i \neq j$ ); although a cutoff is often employed after summing up to just the second-nearest neighbors, it is essential to include more distant neighbors if the model is to avoid unphysical restrictions on  $C_{ijk}$ . For example, if only the first- and second-nearest neighbors are included in a bcc crystal [i.e., the summations are over only the lattice points  $(\pm \frac{1}{2}a, \pm \frac{1}{2}a, \pm \frac{1}{2}a)$ ,  $(\pm a, 0, 0)$ ,  $(0, \pm a, 0)$ , and  $(0, 0, \pm a)$ ], Eqs. (14) and (15) yield  $C_{144} = C_{166}$ . Similarly, for the fcc lattice, inclusion of only the sites  $(\pm \frac{1}{2}a, \pm \frac{1}{2}a, 0)$ ,  $(\pm \frac{1}{2}a, 0, \pm \frac{1}{2}a)$ ,  $(0, \pm \frac{1}{2}a, \pm \frac{1}{2}a)$ ,  $(\pm a, 0, 0)$ ,  $(0, \pm a, 0)$ , and  $(0, 0, \pm a)$  results in  $C_{456} = 0$  in Eq. (16).

### III. CONTRIBUTIONS TO ELASTIC MODULI FROM CENTRAL AND NONCENTRAL INTERACTIONS

If the configurational energy is represented by a pair potential alone [i.e.,  $F(\rho) = 0$ ], inspection of the above equations reveals the Cauchy symmetries  $C_{12} = C_{44}$ ,  $C_{112} = C_{166}$ , and  $C_{144} = C_{123} = C_{456}$ . By employing the EAM, these unrealistic conditions may be avoided. Furthermore, the actual deviations from Cauchy symmetries, often called ‘‘Cauchy discrepancies,’’ may be expressed solely in terms of the noncentral or many-body interactions, which are represented by  $F(\rho)$  and  $f(r)$ . Johnson and Oh<sup>12</sup> made use of this fact in separating  $\phi$  from  $F$  and  $f$  using the second-order Cauchy discrepancy, i.e.,

$$\Omega_0(C_{12} - C_{44}) = F'' \left( \sum \frac{x_1^2 f'}{r} \right)^2. \quad (17)$$

Because we now consider TOEM as well, we can utilize the three third-order Cauchy discrepancies in the derivation of three additional relations between  $F$  and  $f$ :

$$\begin{aligned} \Omega_0(C_{112} - C_{166}) &= F''' \left( \sum \frac{x_1^2 f'}{r} \right)^3 + F'' \left( \sum \frac{x_1^2 f'}{r} \right) \\ &\quad \times \left[ \sum \frac{x_1^4}{r^2} \left( f'' - \frac{f'}{r} \right) \right] + F'' \left( \sum \frac{x_1^2 f'}{r} \right) \\ &\quad \times \left[ \sum \frac{x_1^2 x_2^2}{r^2} \left( f'' - \frac{f'}{r} \right) \right], \end{aligned} \quad (18)$$

$$\begin{aligned} \Omega_0(C_{123} - C_{456}) &= F''' \left( \sum \frac{x_1^2 f'}{r} \right)^3 + 3F'' \left( \sum \frac{x_1^2 f'}{r} \right) \\ &\quad \times \left[ \sum \frac{x_1^2 x_2^2}{r^2} \left( f'' - \frac{f'}{r} \right) \right], \end{aligned} \quad (19)$$

$$\Omega_9(C_{144} - C_{456}) = F'' \left( \sum \frac{x_1^2 f'}{r} \right) \left[ \sum \frac{x_1^2 x_2^2}{r^2} \left( f'' - \frac{f'}{r} \right) \right]. \quad (20)$$

With a little more algebraic manipulation, we separate  $F$  from  $f$ .

Equation (18) plus two times Eq. (20) minus Eq. (19) results in

TABLE I. Physical constants of Al, Cu, Na, and Mo used as input parameters; all data are experimental except for the  $C_{ijk}$  of Na, which are from pseudopotential calculations. Lattice constants (a) are from Ref. 23. Unrelaxed vacancy formation energies ( $E_{IV}$ ) for Al, Cu, Na, and Mo are from Refs. 24, 25, 26, and 27, respectively. Cohesive energies ( $E_{coh}$ ) are from Ref. 28. Second-order moduli ( $C_{ij}$ ) for all metals are from Ref. 29. Third-order moduli ( $C_{ijk}$ ) for Al, Cu, Na, and Mo are from Refs. 30, 31, 32, and 33, respectively.

	Al	Cu	Na	Mo
$a_0$ (Å)	4.05	3.62	4.29	3.15
$E_{IV}$ (eV)	0.67	1.28	0.42	3.1
$E_{coh}$ (eV)	3.34	3.50	1.13	6.81
$C_{11}$ (Mbar)	1.08	1.69	0.0759	4.59
$C_{12}$ (Mbar)	0.62	1.22	0.0633	1.68
$C_{44}$ (Mbar)	0.283	0.753	0.043	1.11
$C_{111}$ (Mbar)	-10.76	-12.71	-0.935	-35.57
$C_{112}$ (Mbar)	-3.15	-8.14	-0.114	-13.33
$C_{123}$ (Mbar)	0.36	-0.50	-0.230	-6.17
$C_{144}$ (Mbar)	-0.23	-0.03	-0.298	-2.69
$C_{166}$ (Mbar)	-3.40	-7.80	-0.172	-8.93
$C_{456}$ (Mbar)	-0.30	-0.95	-0.248	-5.55

$$\begin{aligned} &\Omega_0(2C_{144} + C_{112} - C_{166} - C_{123} - C_{456}) \\ &= F'' \left( \sum \frac{x_1^2 f'}{r} \right) \left[ \sum \frac{x_1^4}{r^2} \left( f'' - \frac{f'}{r} \right) \right]. \end{aligned} \quad (21)$$

Divide each side of Eq. (17) by the respective sides of Eq. (20),

$$\frac{\sum \frac{x_1^2 f'}{r}}{\sum \frac{x_1^2 x_2^2}{r^2} \left( f'' - \frac{f'}{r} \right)} = \frac{C_{12} - C_{44}}{C_{144} - C_{456}}, \quad (22)$$

and by the respective sides of Eq. (21),

$$\frac{\sum \frac{x_1^2 f'}{r}}{\sum \frac{x_1^4}{r^2} \left( f'' - \frac{f'}{r} \right)} = \frac{C_{12} - C_{44}}{2C_{144} + C_{112} - C_{166} - C_{123} - C_{456}}. \quad (23)$$

Equations (22) and (23) provide important information about the character of the electron density function  $f(r)$ . For example, it is evident that a monotonically decreasing function of the form  $f(r) \propto 1/r^\beta$  as used by Johnson and Oh<sup>12</sup> will not, in general, satisfy both relations as this function limits  $f'$  and  $f''$  to negative and positive values, respectively, over the entire range of  $r$ . Such a function will therefore be restricted to negative values in the left-hand sides of *both* Eqs. (22) and (23); apparently, these restrictions are often unrealistic for cubic metals. For example, for Mo and Cu, the actual ratios of second-order to third-order moduli in Eqs. (22) and (23) are both positive; for Al, the ratio in Eq. (22) is positive. (The elastic moduli are listed in Table I.) Here we have provided a strong theoretical justification for employing

an oscillatory model function for  $f(r)$ . It is interesting to note that Wang and Boercker<sup>15</sup> justify their use of such a function on the grounds that it improves the calculated phonon frequency spectra.

As for the contribution to the energy from the central interaction, it turns out that the two second-order shear constants  $\mu=(C_{11}-C_{12})/2$  and  $\mu'=C_{44}$ , which Fuchs<sup>18</sup> was able to isolate using two special strains, and the three third-order shear constants  $(C_{111}-3C_{112}+2C_{123})/8$ ,  $C_{456}$ , and  $(C_{144}-C_{166})/2$ , which were similarly arrived at by Cousins,<sup>19</sup> depend on the central interaction plus a term involving  $dF/d\rho|_e$ , where the subscript denotes the reference state. If we choose  $F(\rho)$  so that  $F'$  at the reference state vanishes, then these five shear constants depend on only the central interaction. The resulting EAM model is said to be of a normalized form; it is known that normalizing an EAM formulation does not result in a loss of generality.<sup>20</sup> The five shear constants, together with the condition for zero pressure in the reference state, give six basic elasticity equations that depend on only the pair potential  $\phi(r)$ :

$$0 = \sum r \phi', \quad (24)$$

$$\Omega_0(C_{11}-C_{12}) = \frac{1}{2} \sum \frac{(x_1^4 - x_1^2 x_2^2)}{r^2} \left( \phi'' - \frac{\phi'}{r} \right), \quad (25)$$

$$\Omega_0 C_{44} = \frac{1}{2} \sum \frac{x_1^2 x_2^2}{r^2} \left( \phi'' - \frac{\phi'}{r} \right), \quad (26)$$

$$\begin{aligned} \Omega_0(C_{111}-3C_{112}+2C_{123}) &= \frac{1}{2} \sum \frac{(x_1^6 - 3x_1^4 x_2^2 + 2x_1^2 x_2^2 x_3^2)}{r^3} \\ &\times \left( \phi''' - 3\frac{\phi''}{r} + 3\frac{\phi'}{r^2} \right), \quad (27) \end{aligned}$$

$$\begin{aligned} \Omega_0(C_{144}-C_{166}) &= \frac{1}{2} \sum \frac{(x_1^2 x_2^2 x_3^2 - x_1^4 x_2^2)}{r^3} \\ &\times \left( \phi''' - 3\frac{\phi''}{r} + 3\frac{\phi'}{r^2} \right), \quad (28) \end{aligned}$$

$$\Omega_0 C_{456} = \frac{1}{2} \sum \frac{x_1^2 x_2^2 x_3^2}{r^3} \left( \phi''' - 3\frac{\phi''}{r} + 3\frac{\phi'}{r^2} \right). \quad (29)$$

One additional property that also depends uniquely on  $\phi$  is the unrelaxed vacancy formation energy  $E_{IV}$ :<sup>20</sup>

$$E_{IV} = -\frac{1}{2} \sum \phi. \quad (30)$$

#### IV. MODEL EAM FUNCTIONS $\phi(r)$ , $f(r)$ , AND $F(\rho)$

In order to illustrate the construction of EAM models for specific metals, based on the formalism outlined in the previous sections, we assume relatively simple forms of the EAM functions  $\phi$  and  $f$ . The pair potential  $\phi(r)$  is taken to be the polynomial

$$\begin{aligned} \phi(r) &= (r-r_m)^4 [b_0 + b_1 r + b_2 r^2 + b_3 r^3 + b_4 r^4 + b_5 r^5 \\ &\quad + b_6 r^6], \quad (31) \end{aligned}$$

where  $r_m$  is the cutoff distance. The factor  $(r-r_m)^4$  ensures the continuities of the pair potential and its first three derivatives at the cutoff distance. With a proper choice of  $r_m$ , the fitting parameters  $b_i$  ( $i=0, \dots, 6$ ) may be determined from Eqs. (24)–(30). As is indicated above,  $r_m$  must be greater than the third-nearest-neighbor distance in order to avoid artificial restrictions on the calculated values of the  $C_{ijk}$ , e.g.,  $C_{144}=C_{166}$  for bcc and  $C_{456}=0$  for fcc. Also mentioned above is the importance of using an oscillatory form for the electron density function; for this purpose, we use

$$f(r) = \frac{[1 + a_1 \cos(\alpha r) + a_2 \sin(\alpha r)]}{r^\beta}, \quad (32)$$

where  $\alpha$  and  $\beta$  are positive parameters. This expression is similar to the form representing Friedel oscillations. But instead of fixing  $\beta$  at 3, it is taken to be a free parameter, and thus may be made large enough that  $f(r)$  converges rapidly; here,  $\beta \equiv 10$ . With an appropriate choice of the parameter  $\alpha$ , the remaining parameters  $a_1$  and  $a_2$  may be determined from Eqs. (22) and (23). Both  $\alpha$  and  $\beta$  are chosen so that  $\rho(a)$ , as defined in Eq. (1b), monotonically decreases with increasing lattice parameter. Physically, this means that the electron density at a reference lattice site decreases as the lattice expands hydrostatically. This requirement ensures that the embedding function is single valued. Although no systematic attempt was made to optimize the values of  $\alpha$  and  $r_m$ , several values of these parameters were tested for each metal. Variation of these two parameters had some small effect on the short-wavelength regions of the phonon frequency spectra; the values reported here gave “visibly pleasing” phonon frequency spectra, in general.

Finally, following the suggestion of Foiles *et al.*,<sup>1</sup> we make use of Rose’s universal equation of state<sup>5</sup> in determining the embedding function  $F(\rho)$ . Substitution of the energy  $E_{EOS}$  from Rose’s equation of state (EOS) for the configurational energy  $E$  in Eq. (1a) yields

$$F(\rho) = E_{EOS}(a^*) - \frac{1}{2} \sum \phi(r), \quad (33a)$$

where

$$E_{EOS}(a^*) = -E_{\text{coh}}(1 + a^* + k a^{*3}) e^{-a^*}, \quad (33b)$$

with

$$a^* = \frac{a - a_0}{a_0 \lambda} \quad \text{and} \quad \lambda = \sqrt{\frac{E_{\text{coh}}}{9 \Omega_0 B}}. \quad (33c)$$

The constants  $a_0$ ,  $E_{\text{coh}}$ ,  $\Omega_0$ , and  $B$  are the lattice parameter, the magnitude of the cohesive energy per atom, volume per atom, and bulk modulus, respectively, at the reference state. The parameter  $k$  depends on the pressure derivative of the bulk modulus at the reference state:

$$k = \frac{\lambda(B' - 1)}{2} - \frac{1}{3}, \quad (34a)$$

TABLE II. Parameters of model EAM functions. The unit of  $b_n$  is eV/Å<sup>(4+n)</sup>.

	Al	Cu	Na	Mo
$\alpha$ (Å <sup>-1</sup> )	4.0	5.0	6.0	4.6
$\beta$	10.0	10.0	10.0	10.0
$a_1$ (eV)	0.402 661 338	-0.290 692 473	-0.099 818 071	-0.388 754 990
$a_2$ (eV)	0.353 591 785	0.478 627 171	-0.006 156 837	0.594 091 434 8
$r_m$ (Å)	6.60	6.92	7.15	5.40
$b_0$	-0.323 461 727	0.183 919 102	-0.041 404 466	56.401 452 096
$b_1$	0.618 464 061	-0.285 826 951	0.063 535 721	-105.785 851 4
$b_2$	-0.468 980 915	0.182 623 033	-0.037 090 867	82.012 737 952
$b_3$	0.182 033 437	-0.061 169 337	0.010 765 683	-33.607 360 49
$b_4$	-0.038 321 001	0.011 322 364	-0.001 640 843	7.670 630 885 2
$b_5$	0.004 154 714	-0.001 104 809	0.000 120 858	-0.923 961 528
$b_6$	-0.000 181 240	0.000 044 742	-0.000 003 088	0.045 855 022 1
$k$	0.0064	0.0621	0.0401	0.0398

$$B' = \left. \frac{dB}{dP} \right|_{P=0} = - \frac{(C_{111} + 6C_{112} + 2C_{123})}{3(C_{11} + 2C_{12})}. \quad (34b)$$

### V. CONSTRUCTION OF EAM MODELS FOR Al, Cu, Na, AND Mo

In this section we examine the applicability of the methodology presented above to the description of cubic metals.

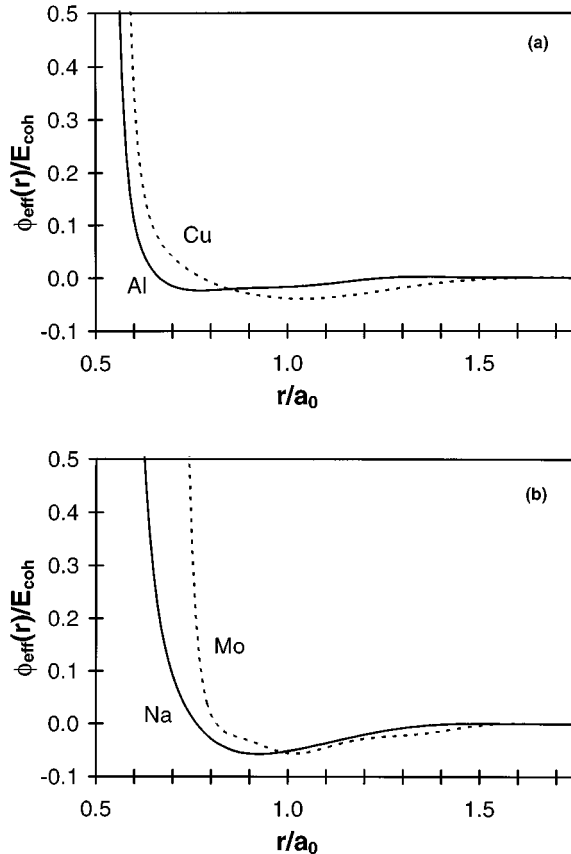


FIG. 1. Variations of the effective pair potentials with interatomic distance: (a) fcc metals Al and Cu (b) bcc metals Na and Mo.

For this purpose we selected four metals that, when considered as an ensemble, provide a broad representation of the characteristic elastic behaviors of cubic metals in general; as a brief digression, this is explained in the remainder of this paragraph. It has been observed that the general elastic response of a metal will depend on the “subgroup” to which the metal belongs. For cubic metals, there are three distinct subgroups<sup>6,21,22</sup> consisting of (i) face-centered-cubic metals, in general, (ii) the body-centered-cubic alkali metals and  $\beta$ -brasses, and (iii) the body-centered-cubic transition metals. For fcc metals, the shear moduli, Young’s moduli, and Poisson’s ratios, respectively, are ordered according to  $\mu' > \mu$ ,  $E_{111} > E_{110} > E_{100}$ , and  $\nu_{110}^{001} > \nu_{100} > \nu_{111} > 0 > \nu_{110}^{1\bar{1}0}$ , where  $E_{hkl}$  is the ratio of stress to strain for uniaxial loading in the crystallographic direction  $[hkl]$ , and  $\nu_{hkl}$  (or  $\nu_{hkl}^{h'k'l'}$ ) is the negative of the ratio of the transverse, isotropic, strain (or, anisotropic, strain in the direction  $[h'k'l']$ ) to the axial strain under the same loading; fcc metals also exhibit upward concavity in their stress-strain relations for  $[100]$  loading, but downward concavity in  $[110]$  and  $[111]$  loading. Aluminum is a notable exception, for which  $\mu' \approx \mu$  and the stated rules of upward concavity and negative Poisson ratio  $\nu_{110}^{1\bar{1}0}$  are vio-

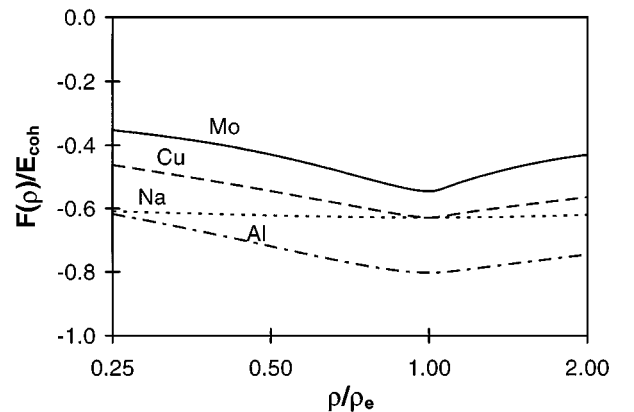


FIG. 2. Variations of the normalized embedding functions with electron density;  $\rho_e$  is the electron density in the reference state. The abscissa scale is logarithmic.

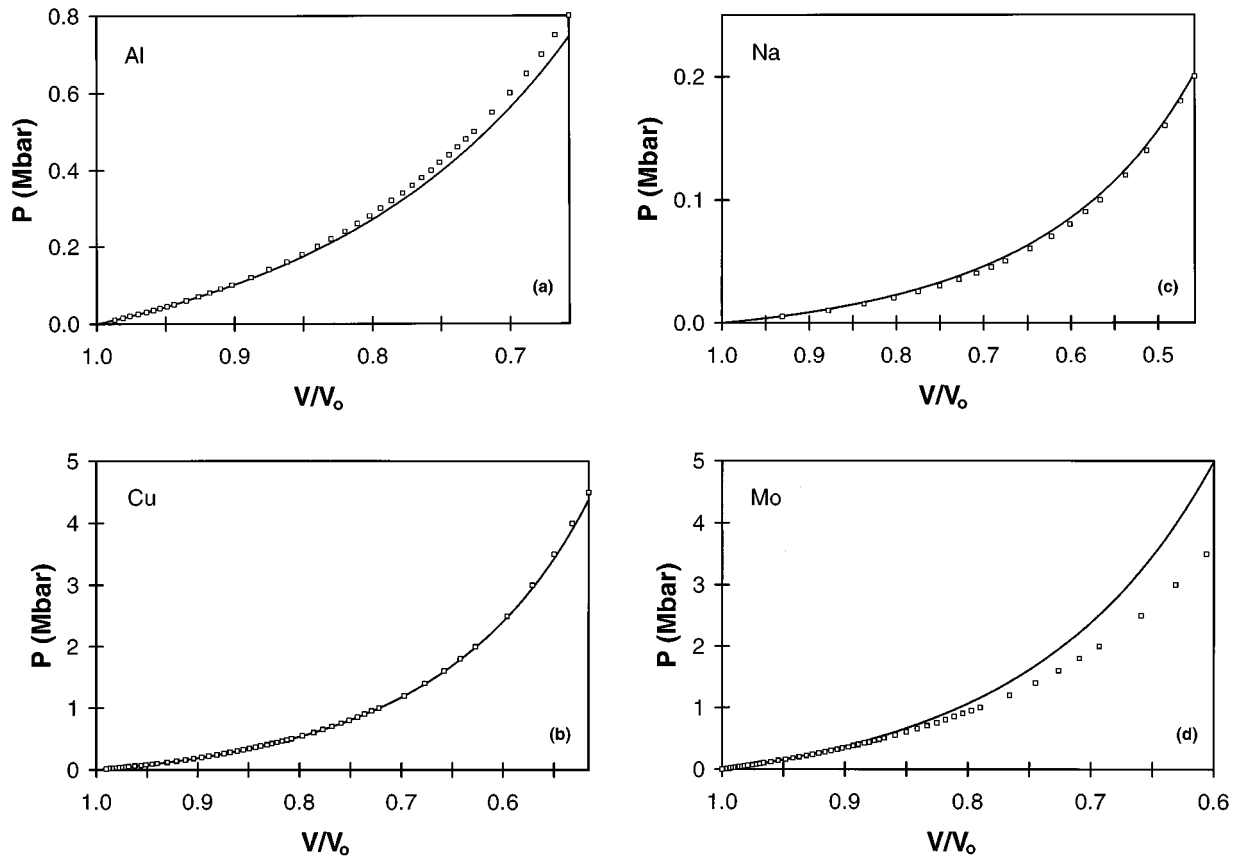


FIG. 3. Compression behavior at 25 °C from Ref. 23 (open squares, experimental; solid line, theoretical): (a) Al, (b) Cu, (c) Na, and (d) Mo.  $P$  is pressure,  $V$  is volume, and  $V_0$  is volume at  $P=0$ .

lated. The elastic response of the bcc alkali metals and  $\beta$ -brasses is also characterized by the orderings  $\mu' > \mu$  (typically,  $\mu/\mu' \sim 0.1$ ),  $E_{111} > E_{110} > E_{100}$ , and  $\nu_{110}^{001} > \nu_{100} > \nu_{111} > 0 > \nu_{110}^{1\bar{1}0}$ , but the uniaxial loading curves are concave upward in [110] loading, and downward in [100] and [111]. Among the six bcc transition metals (V, Nb, Ta, Cr, Mo, and W), with the exception of Ta, the linear elastic trends are ‘‘reversed,’’ i.e.,  $\mu \geq \mu'$ ,  $E_{100} \geq E_{110} \geq E_{111}$ , and  $\nu_{110}^{1\bar{1}0} \geq \nu_{111} \geq \nu_{100} \geq \nu_{110}^{001} > 0$  (the equalities apply to W only). Thus, for modeling purposes, we have selected metals that are typical of each of the subgroups (i.e., Cu for fcc, Na from among the bcc alkalis, and Mo for the bcc transition metals), together with one metal that has anomalous elastic behavior (i.e., Al).

The methodology was then used to construct EAM models of the four cubic metals with the empirical input data that are listed in Table I. The resultant theoretical model parameters are displayed in Table II. The procedure is thus shown to provide EAM models that are capable of incorporating the second- and third-order elastic moduli, as well as the binding energy, lattice parameter, unrelaxed vacancy formation energy, and Rose’s equation of state. The models thus incorporate all of the appropriate, experimentally observed, elastic responses described in the previous paragraph. Figures 1 and 2, respectively, show plots of the effective pair potentials  $\phi_{\text{eff}}(r)$  and the embedding functions. As pointed out by Foiles,<sup>34</sup> the embedding energy part of the total energy in Eq.

(1a) can be considered as  $N$ -body interactions. By performing a Taylor series expansion of  $F(\rho)$  about the reference electron density  $\rho_e$ , one can extract the two-body contribution to the embedding energy. The sum of this contribution and the pair potential is known as the effective pair potential  $\phi_{\text{eff}}(r)$ . Since we set  $F'_e = 0$ , this becomes  $\phi_{\text{eff}}(r) = \phi(r) + F''_e[\rho(r)]^2$ , where the latter term is from the two-body contribution to the embedding energy. The effective pair potential thus characterizes interatomic interactions in an EAM model better than the pair potential alone. Each function  $\phi_{\text{eff}}(r)$  has an intermediate minimum, as expected for a stable crystalline form. Also, as expected,  $\phi_{\text{eff}}(r)$  becomes large and positive at small  $r$ , due to the  $1/r^\beta$  factor in  $f(r)$ , and it approaches zero asymptotically as  $r$  increases.

Theoretical pressure-volume curves according to Rose’s universal equation of state, with the values of  $k$  calculated from Eqs. (34a) and (34b), are compared with experiment in Fig. 3. The curves for Al, Cu, and Na agree very well with experiments, suggesting that the calculated values of  $k$  for

TABLE III. Theoretical structural energy differences.

	Al	Cu	Na	Mo
$E_{\text{bcc}}$ (eV)	-3.2574	-3.4714	-1.1300	-6.8100
$E_{\text{fcc}}$ (eV)	-3.3400	-3.5000	-1.1297	-6.7181
$E_{\text{bcc}} - E_{\text{fcc}}$ (eV)	+0.0826	+0.0286	-0.0003	-0.0919

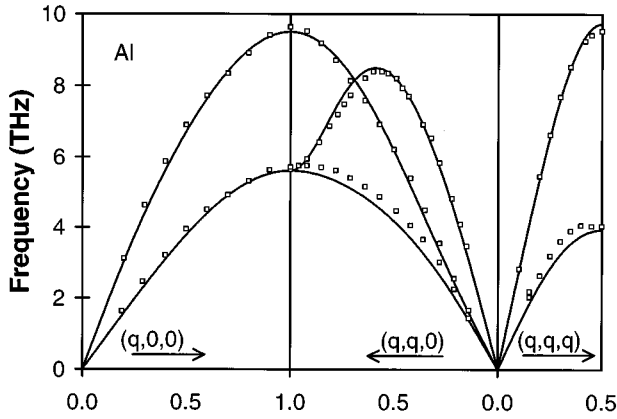


FIG. 4. Experimental and theoretical phonon dispersion curves of Al. Squares represent experimental data at 300 K from Ref. 35.

these metals are accurate. The greater discrepancy in the case of Mo may result from some experimental error in the determination of the TOEM in Ref. 33.

To further explore the efficacy of the present methodology, the energy differences between competing cubic structures and the phonon dispersion curves are calculated and presented in Table III and in Figs. 4–7, respectively. The theoretical phonon frequency spectra are in generally good agreement with experiment. Also, it is satisfying to note that the theoretical cohesive energies are considerably lower for Al and Cu in their fcc configurations and for Mo in its bcc configuration, which are, of course, their experimentally observed structures. The difference in the energies of the bcc and fcc configurations of Na is very small, which again is consonant with experiment, since Na is allotropic (i.e., it transforms from bcc to a faulted fcc structure at low temperature and reverts back to bcc under pressure).

The method presented here is apparently unique in its simplicity and its ability to fit accurately the three second-order and six third-order elastic moduli of cubic crystals. It should be mentioned, however, that other authors have used numerical or optimization techniques to fit EAM models that

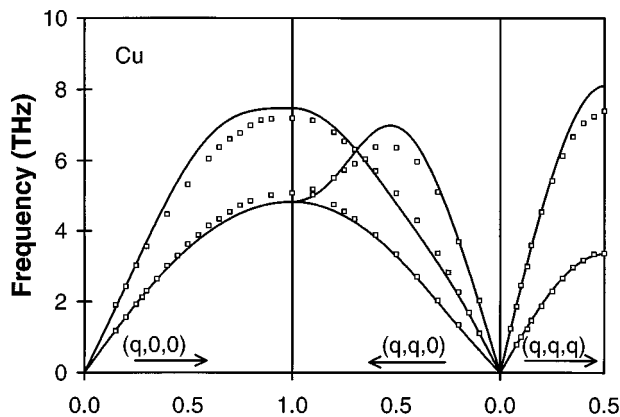


FIG. 5. Experimental and theoretical phonon dispersion curves of Cu. Squares represent experimental data at 296 K from Ref. 36.

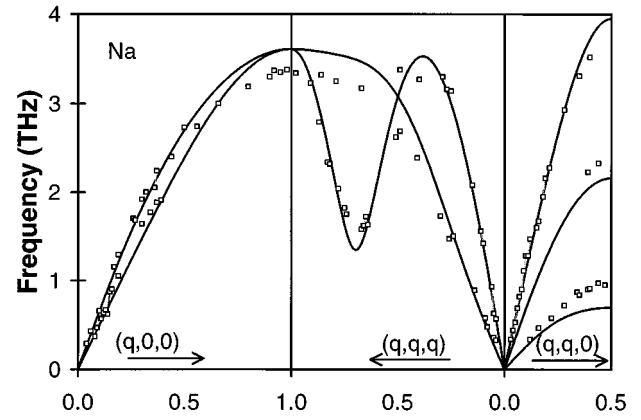


FIG. 6. Experimental and theoretical phonon dispersion curves of Na. Squares represent experimental data at 296 K from Ref. 37.

may implicitly contain third-order elastic moduli, although in such cases it is generally difficult to judge whether the model accurately reproduces all of the second- and third-order moduli. For example, Ercolessi and Adams<sup>39</sup> determined EAM potentials by a nonanalytical optimization method; they include numerous data, such as surface and stacking fault energies, thermal expansions, and defect energies, and their model yields values of the second-order moduli that are within about 10% of the experimental values.

In summary, we have presented an EAM model for metals of cubic symmetry. It allows exact fits to elastic moduli of second and third order, in addition to other empirical data, for a diverse selection of metals, and yields reasonable phonon frequency spectra and energy differences between competing structures. This leads us to speculate that the methodology is able to describe the energetics of most cubic metals reasonably well. Notable exceptions, however, are the metals Cr, Rb, and Ir, for which  $C_{12} < C_{44}$ . Since the curvature of the embedding function is positive (to ensure that the bond strength decreases with increasing coordination<sup>40</sup>), EAM models are applicable only when  $C_{12} > C_{44}$ , as is well known [and may be seen from Eq. (17)]. However, modifi-

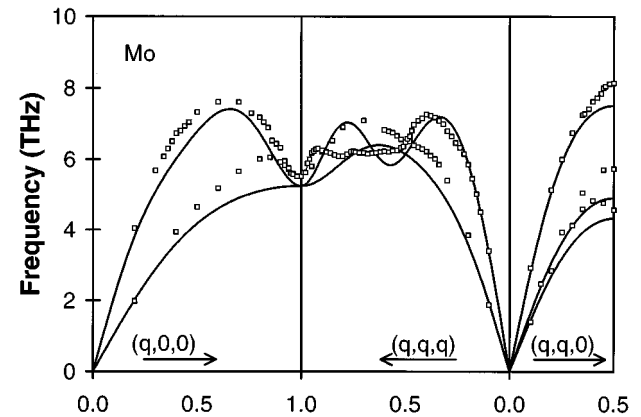


FIG. 7. Experimental and theoretical phonon dispersion curves of Mo. Squares represent experimental data at 300 K from Ref. 38.

cations to the EAM, such as the one used by Baskes,<sup>41</sup> may be employed in the exceptional cases where  $C_{12} < C_{44}$ . While there are still many cubic metals for which the TOEM have not yet been measured, it is hoped that studies such as this will serve as an impetus for further experimental determinations of the higher-order elastic moduli.

#### ACKNOWLEDGMENTS

We would like to acknowledge a fruitful correspondence with Professor James B. Adams at the University of Illinois, Urbana-Champaign. We appreciate financial support from the Academic Senate of the University of California, Santa Barbara.

- 
- <sup>1</sup>S. M. Foiles, M. I. Baskes, and M. S. Daw, *Phys. Rev. B* **33**, 7983 (1986).
- <sup>2</sup>F. Milstein, in *Mechanics of Solids*, edited by H. G. Hopkins and M. J. Sewell (Pergamon, Oxford, 1982), pp. 417–452.
- <sup>3</sup>F. Milstein, J. Marschall, and H. E. Fang, *Phys. Rev. Lett.* **74**, 2977 (1995).
- <sup>4</sup>H. J. P. Van Midden and A. G. B. M. Sasse, *Phys. Rev. B* **46**, 6020 (1992).
- <sup>5</sup>J. H. Rose, J. R. Smith, F. Guinea, and J. Ferrante, *Phys. Rev. B* **29**, 2963 (1984).
- <sup>6</sup>F. Milstein and J. Marschall, *Acta Metall. Mater.* **40**, 1229 (1992).
- <sup>7</sup>F. Milstein and D. J. Rasky, *Phys. Rev. B* **33**, 2341 (1986).
- <sup>8</sup>F. Milstein and A. M. Budek, *Z. Naturforsch.* **42a**, 889 (1987).
- <sup>9</sup>C. S. G. Cousins and J. W. Martin, *J. Phys. F* **8**, 2279 (1978).
- <sup>10</sup>M. S. Daw and M. I. Baskes, *Phys. Rev. B* **29**, 6443 (1984).
- <sup>11</sup>M. S. Daw, S. M. Foiles, and M. I. Baskes, *Mater. Sci. Rep.* **9**, 251 (1993).
- <sup>12</sup>R. A. Johnson and D. J. Oh, *J. Mater. Res.* **4**, 1195 (1989).
- <sup>13</sup>J. B. Adams and S. M. Foiles, *Phys. Rev. B* **41**, 3316 (1990).
- <sup>14</sup>Y. Ouyang and B. Zhang, *Phys. Lett. A* **192**, 79 (1994).
- <sup>15</sup>Y. R. Wang and D. B. Boercker, *J. Appl. Phys.* **78**, 122 (1995).
- <sup>16</sup>M. S. Daw, *Phys. Rev. B* **39**, 7441 (1989).
- <sup>17</sup>K. Brugger, *Phys. Rev.* **133**, A1611 (1964).
- <sup>18</sup>K. Fuchs, *Proc. R. Soc. London A* **153**, 622 (1936).
- <sup>19</sup>C. S. G. Cousins, *Proc. Phys. Soc. London A* **91**, 235 (1967).
- <sup>20</sup>R. A. Johnson, in *Many-Atom Interactions in Solids*, edited by R. M. Nieminen, M. J. Puska, and M. J. Manninen (Springer-Verlag, Berlin, 1990), pp. 85–102.
- <sup>21</sup>F. Milstein and D. J. Rasky, *Philos. Mag. A* **45**, 49 (1982).
- <sup>22</sup>F. Milstein and J. Marschall, *Philos. Mag. A* **58**, 365 (1988).
- <sup>23</sup>*American Institute of Physics Handbook*, 3rd ed. (McGraw-Hill, New York, 1972).
- <sup>24</sup>M. J. Fluss, L. C. Smedskjaer, M. K. Chason, D. G. Legnini, and R. W. Siegel, *Phys. Rev. B* **17**, 3444 (1978).
- <sup>25</sup>R. W. Balluffi, *J. Nucl. Mater.* **69&70**, 240 (1978).
- <sup>26</sup>R. Feder and H. Charbnau, *Phys. Rev.* **149**, 464 (1966).
- <sup>27</sup>K. Maier, M. Peo, B. Saile, H. E. Schaefer, and A. Seeger, *Philos. Mag. A* **40**, 701 (1979).
- <sup>28</sup>Charles Kittel, *Introduction to Solid State Physics*, 4th ed. (Wiley, New York, 1971), p. 96.
- <sup>29</sup>R. F. S. Hearmon, in *Elastic, Piezoelectric and Related Constants of Crystals*, edited by K.-H. Hellwege and A. M. Hellwege, Landolt-Börnstein, New Series, Group III, Vol. 11, Pt. 1 (Springer-Verlag, Berlin, 1979).
- <sup>30</sup>J. F. Thomas, *Phys. Rev.* **175**, 955 (1968).
- <sup>31</sup>Y. Hiki and A. V. Granato, *Phys. Rev.* **144**, 411 (1966).
- <sup>32</sup>R. Srinivasan, *J. Phys. Chem. Solids* **34**, 611 (1973).
- <sup>33</sup>F. F. Voronov, V. M. Prokhurov, E. L. Gromnitskaya, and G. G. Ilina, *Fiz. Met. Metalloved.* **45**, 123 (1978).
- <sup>34</sup>S. M. Foiles, *Phys. Rev. B* **32**, 3409 (1985).
- <sup>35</sup>E. C. Svensson, B. N. Brockhouse, and J. M. Rowe, *Phys. Rev.* **155**, 619 (1967).
- <sup>36</sup>R. Stedman and G. Nilson, *Phys. Rev.* **145**, 492 (1966).
- <sup>37</sup>A. J. Millington and G. L. Squires, *J. Phys. F* **1**, 244 (1971).
- <sup>38</sup>B. M. Powell, P. Martel, and A. D. B. Woods, *Can. J. Phys.* **55**, 1601 (1977).
- <sup>39</sup>F. Ercolessi and J. B. Adams, *Europhys. Lett.* **26**, 583 (1994).
- <sup>40</sup>M. S. Daw, in *Many-Atom Interactions in Solids*, edited by R. M. Nieminen, M. J. Puska, and M. J. Manninen (Springer-Verlag, Berlin, 1990), pp. 48–63.
- <sup>41</sup>M. I. Baskes, *Phys. Rev. B* **46**, 2727 (1992).